

Dynamics in spinor condensates controlled by a microwave dressing field

L. Zhao, J. Jiang, T. Tang, M. Webb, and Y. Liu*

Department of Physics, Oklahoma State University, Stillwater, OK 74078

(Dated: June 11, 2018)

We experimentally study spin dynamics in a sodium antiferromagnetic spinor condensate with off-resonant microwave pulses. In contrast to a magnetic field, a microwave dressing field enables us to explore rich spin dynamics under the influence of a negative net quadratic Zeeman shift q_{net} . We find an experimental signature to determine the sign of q_{net} , and observe harmonic spin population oscillations at every q_{net} except near each separatrix in phase space where spin oscillation period diverges. In the negative and positive q_{net} regions, we also observe a remarkably different relationship between each separatrix and the magnetization. Our data confirms an important prediction derived from the mean-field theory: spin-mixing dynamics in spin-1 condensates substantially depends on the sign of the ratio of q_{net} and the spin-dependent interaction energy. This work may thus be the first to use only one atomic species to reveal mean-field spin dynamics, especially the separatrix, which are predicted to appear differently in spin-1 antiferromagnetic and ferromagnetic spinor condensates.

PACS numbers: 32.60.+i, 67.85.Hj, 03.75.Kk, 03.75.Mn

An atomic Bose-Einstein condensate (BEC) is a state where all atoms have a single collective wavefunction for their spatial degrees of freedom. The key benefit of spinor BECs is the additional spin degree of freedom. Together with Feshbach resonances and optical lattices which tune the interatomic interactions, spinor BECs constitute a fascinating collective quantum system offering an unprecedented degree of control over such parameters as spin, temperature, and the dimensionality of the system [1, 2]. Spinor BECs have become one of the fastest moving research frontiers in the past fifteen years. A number of atomic species have proven to be perfect candidates in the study of spinor BECs, such as $F=1$ and $F=2$ hyperfine spin states of ^{87}Rb atoms [1–7], and $F=1$ hyperfine spin manifolds of ^{23}Na atoms [8–12]. Magnetic fields can induce the quadratic Zeeman energy shift q_{B} . Many interesting phenomena driven by an interplay between q_{B} and the spin-dependent interaction energy c have been experimentally demonstrated in spinor BECs, such as spin population dynamics [1–9], quantum number fluctuation [10, 13], various quantum phase transitions [1, 9, 11, 12], and quantum spin-nematic squeezing [14]. Such systems have been successfully described with a classical two-dimensional phase space [1, 2, 15–17], a rotor model [18], or a quantum model [13, 17].

In this paper, we experimentally study spin-mixing dynamics in a $F=1$ sodium spinor condensate starting from a nonequilibrium initial state, as a result of antiferromagnetic spin-dependent interactions and the quadratic Zeeman energy q_{M} induced by an off-resonant microwave pulse. In contrast to a magnetic field, a microwave dressing field enables us to explore rich spin dynamics under the influence of a negative net quadratic Zeeman energy shift q_{net} . A method to characterize the microwave dressing field is also explained. In both negative and positive q_{net} regions, we observe spin population oscillations

resulted from coherent collisional interconversion among two $|F=1, m_F=0\rangle$ atoms, one $|F=1, m_F=+1\rangle$ atom, and one $|F=1, m_F=-1\rangle$ atom. In every spin oscillation studied in this paper, our data shows that the population of the $m_F=0$ state averaged over time is always larger (or smaller) than its initial value as long as $q_{\text{net}} < 0$ (or $q_{\text{net}} > 0$). This observation provides an experimental signature to determine the sign of q_{net} . We also find a remarkably different relationship between the total magnetization m and a separatrix in phase space where spin oscillation period diverges: the position of the separatrix moves slightly with m in the positive q_{net} region, while the separatrix quickly disappears when m is away from zero in the negative q_{net} region. Our data confirms an important prediction derived by Ref. [17]: the spin-mixing dynamics in $F=1$ spinor condensates substantially depends on the sign of $R = q_{\text{net}}/c$. This work may thus be the first to use only one atomic species to reveal mean-field spin dynamics, especially the separatrix, which are predicted to appear differently in $F=1$ antiferromagnetic and ferromagnetic spinor condensates.

Similar to Ref. [1, 16], we take into account the conservation of m and the total atom number. Because no spin domains and spatial modes are observed in our system, the single spatial mode approximation (SMA), in which all spin states have the same spatial wavefunction, appears to be a proper theoretical model to understand our data. Spin-mixing dynamics in a $F=1$ spinor BEC can thus be described with a two-dimensional (ρ_0 vs θ) phase space, where the fractional population ρ_{m_F} and the phase θ_{m_F} of each m_F state are independent of position. The BEC energy E and the time evolution of ρ_0 and θ may be expressed as [1, 16]

$$E = q_{\text{net}}(1 - \rho_0) + c\rho_0[(1 - \rho_0) + \sqrt{(1 - \rho_0)^2 - m^2} \cos \theta],$$
$$\dot{\rho}_0 = -(2/\hbar)\partial E/\partial \theta, \quad \dot{\theta} = (2/\hbar)\partial E/\partial \rho_0. \quad (1)$$

Here $q_{\text{net}} = q_{\text{B}} + q_{\text{M}}$, $\theta = \theta_{+1} + \theta_{-1} - 2\theta_0$ is the relative phase among the three m_F spin states, and \hbar is the reduced Planck constant. The induced linear Zeeman shift

* yingmei.liu@okstate.edu

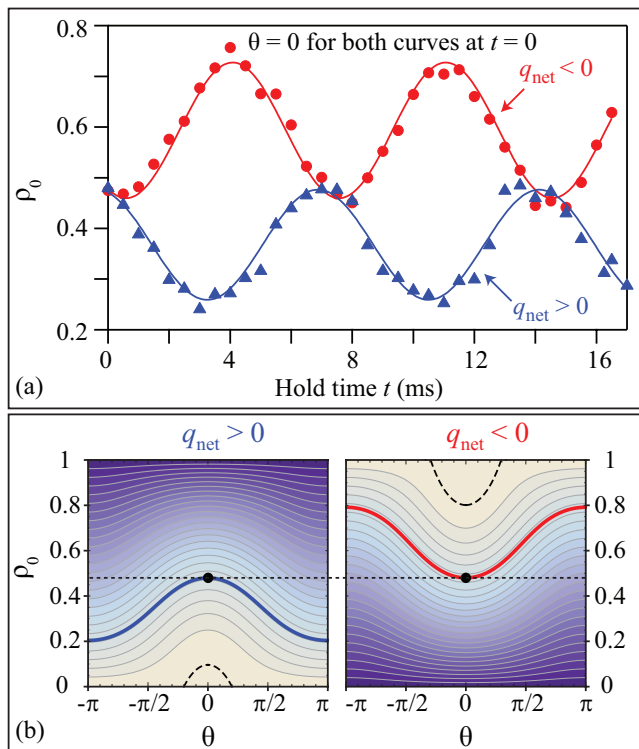


FIG. 1. (color online)(a). Time evolutions of ρ_0 at $q_{\text{net}}/h = +93 \text{ Hz} > 0$ (solid blue triangles) and $q_{\text{net}}/h = -83 \text{ Hz} < 0$ (solid red circles) with $m = 0$ and $c/h = 52 \text{ Hz}$. It is important to note that the two curves start from the same initial state with $\theta|_{t=0} = 0$. Solid lines are sinusoidal fits to the data. (b) Equal-energy contour plots based on Eq. 1 for the two experimental conditions shown in Fig. 1(a), i.e., $q_{\text{net}} > 0$ (left) and $q_{\text{net}} < 0$ (right). The heavy solid blue and red lines represent the energy of the above two experimental conditions, respectively. The dotted black horizontal line is to emphasize the fact that the above two experiments start with the same initial state which is marked by the solid black circles. Dashed black lines represent the energy of the separatrix between the running and oscillatory phase solutions. Darker colors correspond to lower energies.

remains the same during the collisional spin interconversion and is thus ignored. The spin-dependent interaction energy is $c = c_2 \langle n \rangle$, where $\langle n \rangle$ is the mean BEC density and c_2 is the spin dependent interaction coefficient. The total magnetization is $m = \rho_{+1} - \rho_{-1}$. It is well known that $q_B \propto B^2 > 0$, and $c_2 > 0$ (or $c_2 < 0$) in $F=1$ ^{23}Na (or ^{87}Rb) spinor BECs. Spin-dynamics in $F=1$ antiferromagnetic and ferromagnetic spinor BECs have been studied in magnetic fields where $q_{\text{net}} > 0$ with ^{23}Na and ^{87}Rb atoms, respectively [1]. A few methods have been explored for generating a negative quadratic Zeeman shift, such as via a microwave dressing field [1, 11, 19–21] or through a linearly polarized off-resonant laser beam [22]. In this paper, we choose the first method.

The experimental setup is similar to that illustrated in our previous work [23]. Hot ^{23}Na atoms are slowed by a spin-flip Zeeman slower, captured in a standard magneto-

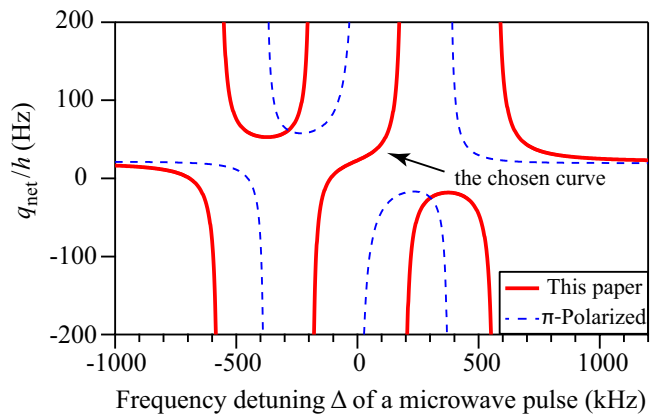


FIG. 2. (color online) q_{net} as a function of Δ . The residual magnetic field is $B=270 \text{ mG}$. Dashed blue lines and solid red lines represent the predictions derived from Eq. 2 when the microwave pulse is purely π -polarized and when the pulse has a specially-chosen polarization, respectively (see text). In this paper, Δ is tuned within the range of -190 kHz to 190 kHz .

optical trap, cooled through a polarization gradient cooling process to $40 \mu\text{K}$, and loaded into a crossed optical dipole trap originating from a linearly-polarized high power IR laser at 1064 nm . After an optimized 6 s forced evaporative cooling process, a pure $F=1$ BEC of 1×10^5 sodium atoms is created. We can polarize atoms in the $F=1$ BEC fully to the $|F=1, m_F=-1\rangle$ state by applying a weak magnetic field gradient during the first half of the forced evaporation (or fully to the $|F=1, m_F=0\rangle$ state by adding a very strong magnetic bias field during the entire 6 s forced evaporation). We then ramp up a small magnetic bias field with its strength B being 270 mG , while turning off the field gradient. An rf-pulse resonant with the linear Zeeman splitting is applied to prepare an initial state with any desired combination of the three m_F states. To generate sufficiently large q_{net} with off-resonant microwave pulses, a microwave antenna designed for a frequency near the $|F=1\rangle \leftrightarrow |F=2\rangle$ transition is placed a few inches above the center of the magneto-optical trap, and connected to a function generator outputting a maximum radiation power of 10 W . After various hold time t in the optical dipole trap, populations of the multiple spin states are then measured via the standard absorption imaging preceded by a 3 ms Stern-Gerlach separation and a 7 ms time of flight.

We observe spin oscillations at every given value of q_{net} within a wide range, i.e., $-240 \text{ Hz} \leq q_{\text{net}}/h \leq 240 \text{ Hz}$. Here h is the Planck constant. Typical time evolutions of ρ_0 starting with the same nonequilibrium initial state at a negative and a positive q_{net} are shown in Fig. 1(a). We find that these evolutions can be well fit by sinusoidal functions of the similar oscillation period T and amplitude A . On the other hand, our data in Fig. 1(a) shows that the value of $\langle \rho_0 \rangle$ is drastically different in the two spin oscillations: $\langle \rho_0 \rangle > \rho_0|_{t=0}$ as long as $q_{\text{net}} < 0$, while $\langle \rho_0 \rangle < \rho_0|_{t=0}$ if $q_{\text{net}} > 0$. Here $\langle \rho_0 \rangle$ is the average

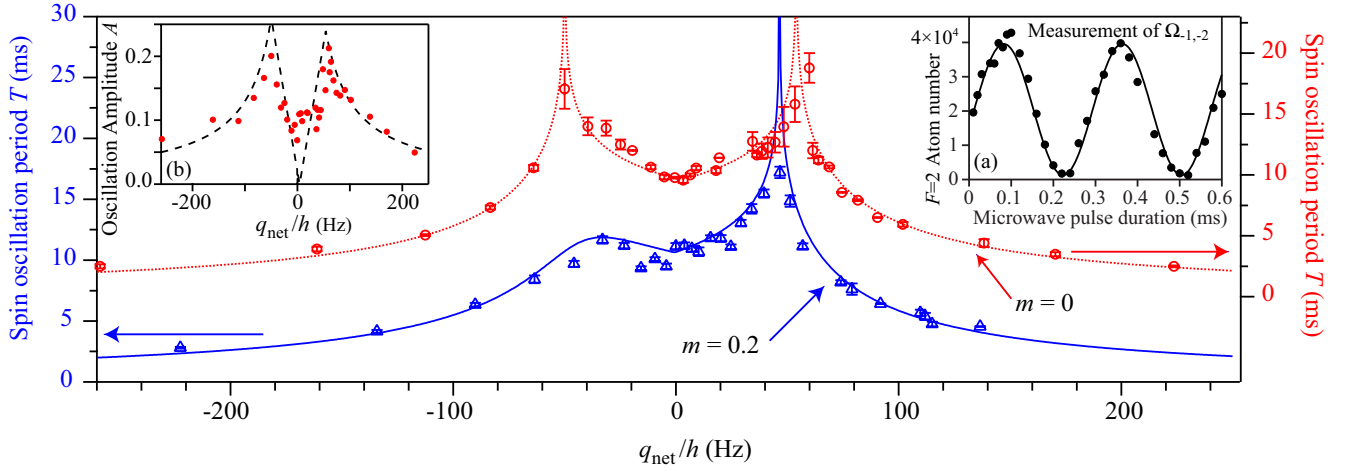


FIG. 3. (color online) The spin oscillation period as a function of q_{net} for $m = 0$ (open red circles) and $m = 0.2$ (open blue triangles). The lines are fits based on Eq. 1, which yield the fit parameters: $\rho_0|_{t=0} = 0.48$, $\theta|_{t=0} = 0$, and $c/h = 52$ Hz for $m = 0$; and $\rho_0|_{t=0} = 0.48$, $\theta|_{t=0} = 0$, and $c/h = 47$ Hz for $m = 0.2$. The fit parameters are within the 5% uncertainty of our measurements. Note the different scales of the left and right vertical axes. Inset (a): the number of $F = 2$ atoms excited by a resonant microwave pulse as a function of the pulse duration. The solid line is a sinusoidal fit to extract the on-resonance Rabi frequency $\Omega_{-1,-2}$. Inset (b): amplitudes A of spin oscillations shown in the main figure as a function of q_{net} at $m = 0$. The dashed black line is a fit based on Eq. 1 with the same set of fit parameters as that applied in the main figure.

value of ρ_0 over time in a spin oscillation and $\rho_0|_{t=0}$ is the initial value of ρ_0 . This phenomenon is observed at every value of q_{net} when spin oscillations start with the same initial state, although the period T and amplitude A change with q_{net} . The above observations agree well with predictions from the mean-field SMA theory (i.e., Eq. 1) as shown by the heavy solid lines in Fig. 1(b): ρ_0 is limited between $(\rho_0|_{t=0} - 2A)$ and $\rho_0|_{t=0}$ at $q_{\text{net}} > 0$, while it is restricted between $\rho_0|_{t=0}$ and $(\rho_0|_{t=0} + 2A)$ at $q_{\text{net}} < 0$. We can thus use the phenomenon to conveniently determine the sign of q_{net} , i.e., by comparing the value of $\langle \rho_0 \rangle$ of a spin oscillation to the value of $\rho_0|_{t=0}$.

On the other hand, the exact value of q_{net} is carefully calibrated based on Eq. 2 with a few experimental parameters, such as the polarization and frequency of a microwave pulse. Every microwave pulse used in this paper is detuned by Δ from the $|F = 1, m_F = 0\rangle \leftrightarrow |F = 2, m_F = 0\rangle$ transition. A purely π -polarized microwave pulse has been a popular choice in some publications [1, 11, 19–21]. However, the microwave pulse used in this paper has a specially-chosen polarization in order to easily access every positive and negative value of q_{net} just by continuously tuning Δ , as shown in Fig. 2. We define k as 0 or ± 1 for a π or a σ_{\pm} polarized microwave pulse, respectively. For a given polarization k , the allowed transition is $|F = 1, m_F\rangle \leftrightarrow |F = 2, m_F + k\rangle$ and its on-resonance Rabi frequency is $\Omega_{m_F, m_F+k} \propto \sqrt{I_k} C_{m_F, m_F+k}$, where C_{m_F, m_F+k} is the Clebsch-Gordan coefficient of the transition and I_k is the intensity of this purely polarized microwave pulse. We also define $\Delta_{m_F, m_F+k} = \Delta - [(m_F + k)/2 - (-m_F/2)]\mu_B B$ as the frequency detuning of the microwave pulse with respect to the $|F = 1, m_F\rangle \rightarrow |F = 2, m_F\rangle$ transition, where

μ_B is the Bohr magneton. Similar to Refs. [19, 21], we express the value of q_{net} as

$$\begin{aligned} q_{\text{net}} &= q_B + q_M \\ &= aB^2 h + (\delta E|_{m_F=1} + \delta E|_{m_F=-1} - 2\delta E|_{m_F=0})/2, \\ \delta E|_{m_F} &= \frac{h}{4} \sum_k \frac{\Omega_{m_F, m_F+k}^2}{\Delta_{m_F, m_F+k}}, \end{aligned} \quad (2)$$

where $a \approx 277$ Hz/G² (or $a \approx 71$ Hz/G²) for $F=1$ ²³Na (or ⁸⁷Rb) atoms. Due to the limited power of our microwave function generator, we obtain a desired value of q_{net} by choosing a proper Δ within the range of -190 kHz to 190 kHz at a fixed intensity, as shown in Fig. 2. The on-resonance Rabi frequencies of our microwave pulses are $\Omega_{-1,-2} = 3.6$ kHz, $\Omega_{0,-1} = 2.1$ kHz, $\Omega_{1,0} = 1.5$ kHz, $\Omega_{-1,-1} = \Omega_{0,0} = \Omega_{1,1} = 0$, $\Omega_{-1,0} = 1.6$ kHz, $\Omega_{0,1} = 2.8$ kHz, and $\Omega_{1,2} = 4.0$ kHz. Another advantage of choosing such microwave pulses is to conveniently place the microwave antenna on our apparatus without blocking optical components. In order to ensure an accurate calibration of q_{net} based on Eq. 2, we measure Ω_{m_F, m_F+k} everyday by monitoring the number of atoms excited by a resonant microwave pulse to the $F=2$ state as a function of the pulse duration. A typical example of the Rabi frequency measurement is shown in the inset (a) in Fig. 3.

The time evolution of ρ_0 is fit by a sinusoid to extract the spin oscillation period T and amplitude A at a given q_{net} , as shown in Fig. 1(a). The value of T as a function of q_{net} is then plotted in Fig. 3 for $m = 0$ and $m = 0.2$, which demonstrates two interesting results. First, when $m = 0$, the spin oscillation is harmonic except near the critical values (i.e., $q_{\text{net}}/h = \pm 52$ Hz) where the period diverges. This agrees with the predictions derived from

Eq. 1, as shown by the dotted red line in Fig. 3. The energy contour E_{sep} where the oscillation becomes anharmonic is defined as a separatrix in phase space. A point on the separatrix satisfies the equation $\dot{\rho}_0 = \dot{\theta} = 0$ according to the mean-field SMA theory. In fact for our sodium system with $c > 0$, $E_{\text{sep}} = q_{\text{net}}$ for $q_{\text{net}} > 0$, while $E_{\text{sep}} = 0$ at $m = 0$ for $q_{\text{net}} < 0$. Figure 3 shows that the T vs q_{net} curve is symmetric with respect to the $q_{\text{net}} = 0$ axis at $m = 0$. The period T decreases rapidly with increasing $|q_{\text{net}}|$ when $|q_{\text{net}}|$ is large, which corresponds to the “Zeeman regime” with running phase solutions. In the opposite limit, the period only weakly depends on $|q_{\text{net}}|$, which represents the “interaction regime” with oscillatory phase solutions. Here $|q_{\text{net}}|$ is the absolute value of q_{net} . The value of θ is (or is not) restricted in the regions with oscillatory (or running) phase solutions. Refs [8, 9] reported observations of the similar phenomena for $q_{\text{net}} > 0$ with a $F=1$ antiferromagnetic spinor condensate, however, they did not access the negative q_{net} region.

Figure 3 also demonstrates a remarkably different relationship between the total magnetization m and the separatrix in phase space: the position of the separatrix moves slightly with m in the positive q_{net} region, while the separatrix quickly disappears when m is away from zero in the negative q_{net} region. Good agreements between our data and the mean-field SMA theory are shown in the inset (b) and the main figure in Fig. 3. Interestingly, we find that the spin dynamics which appear in our antiferromagnetic sodium system in the negative q_{net} region exactly mimic what is predicted to occur in a ferromagnetic spinor condensate in the positive q_{net} region [16, 17]. Note that $R = q_{\text{net}}/c$ is negative in both of these two cases. This observation confirms an important prediction made by Ref. [17]: the spin-mixing dynamics in $F=1$ spinor condensates substantially depends on the

sign of R . As a matter of fact, our results in the negative q_{net} region are similar to those reported with a $F=1$ ferromagnetic ^{87}Rb spinor condensate in magnetic fields where $q_{\text{net}} > 0$ [1, 3]. Although the relationship between the separatrix and m in the ferromagnetic Rb system has not been experimentally explored yet, our data in Fig. 3 can be extrapolated to understand this relationship. This paper may thus be the first to use only one atomic species to reveal mean-field spin dynamics, especially the separatrix, which are predicted to appear differently in $F=1$ antiferromagnetic and ferromagnetic spinor condensates.

In conclusion, we have experimentally studied spin dynamics in a sodium spinor condensate controlled by a microwave dressing field. In both negative and positive q_{net} regions, we have observed harmonic spin oscillations and found that the sign of q_{net} can be determined by comparing $\langle \rho_0 \rangle$ to $\rho_0|_{t=0}$. Our data also demonstrates that the position of the separatrix in phase space moves slightly with m in the positive q_{net} region, while the separatrix quickly disappears when m is away from zero in the negative q_{net} region. Our data confirms that the spin-mixing dynamics in $F=1$ spinor condensates substantially depends on the sign of $R = q_{\text{net}}/c$. This paper may thus be the first to use only one atomic species to reveal mean-field spin dynamics and the separatrix, which are predicted to appear differently in $F=1$ antiferromagnetic and ferromagnetic spinor condensates. In addition, the microwave dressing field is able to completely cancel out q_B induced by ambient stray magnetic fields. This allows us to study interesting but unexplored phenomena at $q_{\text{net}} = 0$, for example, realizing a maximally entangled Dicke state with sodium spinor condensates [24].

We thank the Army Research Office, Oklahoma Center for the Advancement of Science and Technology, and Oak Ridge Associated Universities for financial support. M.W. thanks the Niblack Research Scholar program.

-
- [1] D. M. Stamper-Kurn and M. Ueda, *Rev. Mod. Phys.* **85**, 1191 (2013).
 - [2] Y. Kawaguchi and M. Ueda, *Phys. Rep.* **520**, 253 (2012).
 - [3] M.-S. Chang, Q. Qin, W. Zhang, L. You, and M. S. Chapman, *Nature Physics* **1**, 111 (2005).
 - [4] A. Widera, F. Gerbier, S. Fölling, T. Gericke, O. Mandel, and I. Bloch, *New Journal of Physics* **8**, 152 (2006).
 - [5] J. Kronjäger, C. Becker, P. Navez, K. Bongs, and K. Sengstock, *Phys. Rev. Lett.* **97**, 110404 (2006).
 - [6] H. Schmaljohann, M. Erhard, J. Kronjäger, M. Kottke, S. van Staa, L. Cacciapuoti, J. J. Arlt, K. Bongs, and K. Sengstock, *Phys. Rev. Lett.* **92**, 040402 (2004).
 - [7] T. Kuwamoto, K. Araki, T. Eno, and T. Hirano, *Phys. Rev. A* **69**, 063604 (2004).
 - [8] A. T. Black, E. Gomez, L. D. Turner, S. Jung, and P. D. Lett, *Phys. Rev. Lett.* **99**, 070403 (2007).
 - [9] Y. Liu, S. Jung, S. E. Maxwell, L. D. Turner, E. Tiesinga, and P. D. Lett, *Phys. Rev. Lett.* **102**, 125301 (2009).
 - [10] Y. Liu, E. Gomez, S. E. Maxwell, L. D. Turner, E. Tiesinga, and P. D. Lett, *Phys. Rev. Lett.* **102**, 225301 (2009).
 - [11] E. M. Bookjans, A. Vinit, and C. Raman, *Phys. Rev. Lett.* **107**, 195306 (2011).
 - [12] D. Jacob, L. Shao, V. Corre, T. Zibold, L. De Sarlo, E. Mimoun, J. Dalibard, and F. Gerbier, *Phys. Rev. A* **86**, 061601 (2012).
 - [13] L. Chang, Q. Zhai, R. Lu, and L. You, *Phys. Rev. Lett.* **99**, 080402 (2007).
 - [14] C. D. Hamley, C. S. Gerving, T. M. Hoang, E. M. Bookjans, and M. S. Chapman, *Nature Physics* **8**, 305 (2012).
 - [15] W. Zhang, S. Yi, and L. You, *New Journal of Physics* **5**, 77 (2003).
 - [16] W. Zhang, D. L. Zhou, M.-S. Chang, M. S. Chapman, and L. You, *Phys. Rev. A* **72**, 013602 (2005).
 - [17] A. Lamacraft, *Phys. Rev. A* **83**, 033605 (2011).
 - [18] R. Barnett, J. D. Sau, and S. Das Sarma, *Phys. Rev. A* **82**, 031602 (2010).
 - [19] F. Gerbier, A. Widera, S. Fölling, O. Mandel, and I. Bloch, *Phys. Rev. A* **73**, 041602(R) (2006).
 - [20] S. R. Leslie, J. Guzman, M. Vengalattore, J. D. Sau, M.

- L. Cohen, and D. M. Stamper-Kurn, Phys. Rev. A **79**, 043631 (2009).
- [21] Sabrina R. A. Leslie, Ph.D. thesis (2008).
- [22] L. Santos, M. Fattori, J. Stuhler, and T. Pfau, Phys. Rev. A **75**, 053606 (2007).
- [23] J. Jiang, L. Zhao, M. Webb, N. Jiang, H. Yang, and Y. Liu, Phys. Rev. A **88**, 033620 (2013).
- [24] Z. Zhang and L.-M. Duan, arXiv:1308.2318 (2013).